Journal of Theoretical and Applied Information Technology
31st January 2019. Vol.97. No 2

ISSN: 1992-8645 www.jatit.org E-ISSN: 1817-3195

DIAGNOSES OF BREAST CANCER IN HISTOPATHOLOGICAL IMAGES BASED ON DEEP LEARNING

MOHAMAD MAHMOUD AL RAHHAL

Information Science, College of Applied Computer Science, King Saud University, Riyadh, KSA

E-mail: mmalrahhal@ksu.edu.sa

ABSTRACT

Detection and classification of cancer in histopathological images is one of the biggest challenges for oncologists. Deep learning approaches have proved to be very valuable tools in dealing with histopathological images, and the results obtained from such approaches help the oncologists in the diagnosis of breast cancer. In this paper, we propose a deep convolutional neural network approach to generate a robust feature representation from histopathological images. We employed three different pre-trained models, namely: Vgg_m, VeryDeep_16, and Googlenet, and the method has been evaluated in two different scenarios. In the first scenario (magnification dependent), we train networks separately depending on image magnification (40x, 100x, 200x, and 400x). In the second scenario, we utilize all available data in the training set independent of magnification. For both scenarios, we demonstrate superior results at both patient and image levels compared to state of the art methods

Keywords: *Convolutional Neural Network, CNN, Histopathological Images, Imagenet, Classification, Breast Cancer.*

1. INTRODUCTION

Machine learning is a common type of Artificial Intelligence (AI) used for processing big data. ML involves self-adaptive algorithms that learn from data and apply what they learn to make decisions. These algorithms are learning more from experience and new data.

Deep learning is a subset of machine learning and has been one of the hottest topics of research over the last two decades. deep learning is based on learning data representations, which means that representations needed for feature extraction or classification are automatically found from raw data that is given as an input. Deep learning uses multiple layers/levels to process data non-linearly. It begins with raw data, and then each layer uses the output of the previous layer as an input [1]. The learning strategies for deep learning can be supervised or unsupervised learning.

Deep learning can generate new features from limited features of training data. Also, the unsupervised technique is one of its advantages that makes the system smarter.

Deep learning has found massive solutions for different applications, such as speech recognition [2], [3], face recognition [4], [5], computer vision, and natural language processing. Deep learning also provides accurate results when applied to medical images. Applying the deep learning approach is considered as a key method and a trend for current and future medical applications such as breast cancer diagnosis and classification of masses [6]–[16], abdominal adipose tissues extraction [17], classification of brain cancer [18]–[21], skeletal bone age assessment in X-ray images [22], and arrhythmia detection and analysis in ECG signals [23]–[25].

Due to the proliferation of cancer, which is one of the major cause of mortality around the world, we used deep learning approach for breast cancer detection and classification. Breast cancer is most common in women as reported by the World Health Organization [26].

Commonly, screening protocol involves mammography to determine suspect areas of the breast, which is followed by a biopsy of potentially cancerous areas in order to distinguish whether the suspect region is malignant or benign [28], [29].

ISSN: 1992-8645 www.jatit.org E-ISSN: 1817-3195

In [27], a CAD system for breast cancer diagnosis is proposed, which can classify mass lesions using deep learning techniques. Their method is based on deep convolutional neural networks (CNNs). Their proposed method involves a preprocessing step for extracting the benign and malignant lesions using the coordinates provided with each dataset to crop the bounding box of the lesions automatically. After applying preprocessing and normalization steps, they applied deep learning with data augmentation.

In this context, automatic analysis for histopathological images plays a substantial role in assisting diagnosis. A nuclei segmentation was proposed in [30] in order to categorize lesions as benign or malignant. In [31], a breast cancer image classification system was proposed, where the authors adopted four different classifiers trained with 25-dimensional feature vectors; with 737 images, they achieved an accuracy of 98%. A diagnostic system for breast cancer based on the nuclei segmentation of cytological images was suggested in [32], where different machine learning models, such as neural networks and support vector machines, were adopted, and reported accuracies ranged from 76% to 94% with a dataset of 92 images.

On the other hand, the remarkable advent of powerful processing facilities has benefited computer vision and machine learning communities at large. One of the by-products in this sense is deep learning, which can be regarded as an advantageous breakthrough. A particular case that has emerged in very recent years is CNNs, which have benefited computer vision at large.

Deep learning uses multiple layers/levels to process data non-linearly. It begins with raw data, and then each layer uses the output of the previous layer as input.

In this work, we propose a breast cancer diagnosis approach based on CNN models to generate a robust feature representation from histopathological training images. We employed three different pre-trained models: Vgg_m, VeryDeep_16, and Googlenet.

The remainder of this paper is organized as follows. The proposed methodology is described in Section II, experimental results are given in Section III, and conclusions are provided in Section VI.

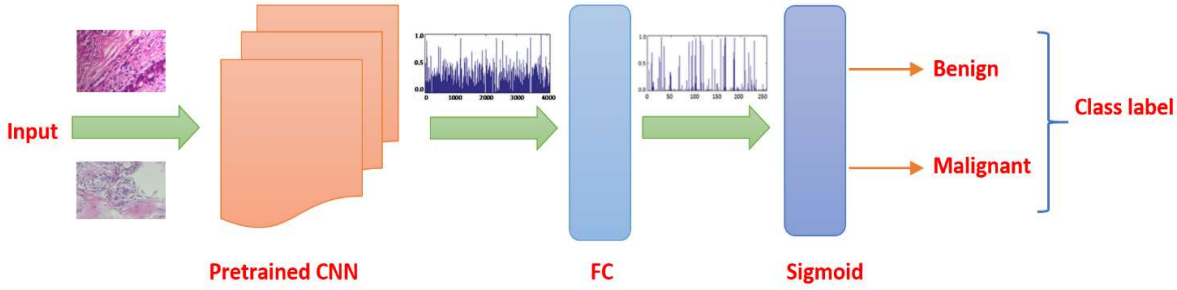

Figure 1. Flowchart of the proposed approach.

2. PROPOSED METHODOLOGY

Let us consider $D^{(s)} = \{\boldsymbol{x}_i, \boldsymbol{y}_i\}_{i=1}^{n_s}$ as the labeled source data and $y_i \in \{1,2\}$ as its corresponding class label, where the value 1 represents benign and 2 represents malignant. Similarly, let $D^{(t)} = \{\boldsymbol{x}_j\}_{j=1}^{n_t}$ be unseen target data. Our methodology consists of two phases, as shown in Figure 1.

2.1 Phase 1

We used a pre-trained CNN for automatic feature extraction; it consists of multiple layers to deal with specific problems [33]–[35]. Generally, four layers are used to construct deep CNNs: a convolutional layer, a pooling layer, a non-linear activation layer, and a fully connected layer. Features are extracted in the first three layers, and then the fully connected layer is used for classification.

The main layer of the CNN is the convolutional layer, which is composed of a

ISSN: 1992-8645 www.jatit.org E-ISSN: 1817-3195

collection of neurons or filters. Each neuron is spatially small (in height and width), but it slides across the input image in order to generate a feature map or activation map. Feature maps, which are the output of this layer, are then forwarded to the next layer, which is a non-linear activation function such as the rectified linear unit. The next layer (normalization layer) is then fed with the output of the activation layer to assist in generalization.

The responsibility of the pooling layer is to control for overfitting. This layer is typically used straight after the convolutional layer by taking every feature map, and then generating another more condensed feature map.

A fully connected layer is the last layer of the CNN network. Each neuron within one fully connected layer is connected to all neurons in the previous layer. Finally, classification is done by adding a sigmoid layer at the end of the network, and then by using back-propagation, the weights of the CNN are learned.

In this work, we aim to exploit the power of CNN models to represent images by taking the output of the last fully connected layer before the classification layer. That is, for each input image $\mathbf{I}_i$, we generate a CNN feature representation vector $\boldsymbol{x}_i \in \Re^d$ of dimension

$$\boldsymbol{x}_i = f_{L-1}^{\mathrm{CNN}}\left(\dots f_2^{\mathrm{CNN}}\left(f_1^{\mathrm{CNN}}(\mathbf{I}_i)\right)\right), \qquad i = 1, \dots, n_s \quad (1)$$

where n_s represent the number of labelled source images, $f_j^{\mathrm{CNN}}, j = 1, \dots, L-1$ defines the functions of different CNN layers, and L is the number of layers in the network.

2.2 Phase 2

This phase is termed the classification phase; it manages the outputs of the previous phase (CNN feature vectors) by feeding them as an input to an extra network connected to the highest of pre-trained CNN, as shown in Fig 1. This extra network is made from 2 fully-connected layers; the first is a hidden layer, and the other is a sigmoid layer used for binary classification. The hidden layer accepts $\boldsymbol{x}_i$ as an input and represents it through the nonlinear activation function f as follows:

$$\boldsymbol{h}_i^{(1)} = f(\boldsymbol{W}^{(1)}\boldsymbol{x}_i), \quad (2)$$

where $\boldsymbol{h}_i^{(1)} \in \Re^{d^{(1)}}$ is of dimension $d^{(1)}$, an $\boldsymbol{W}^{(1)} \in \Re^{d^{(1)} \times d}$ is the mapping weight matrix. For a nonlinear activation function, a sigmoid function is used: $f(s) = 1/(1 + \exp(-\mathrm{s}))$.

To avoid overfitting and increase its generalization ability, we used the dropout technique used in [36]. The aim of this technique is to drop nodes from the hidden layer throughout the training phase. To reduce the complexity of the network, this technique randomly removes nodes from the original fully-connected network.

The weights learned represent the complete network structure, as described in [37].

3. EXPERIMENTAL RESULTS

3.1 Dataset Description

In order to assess the performances of the proposed technique, we used the Breast Cancer Histopathological Image Classification (BreakHis) dataset, which was established recently in [33]; it contains 109 microscopic images of breast cancer (malignant and benign) collected from 82 patients under four magnification factors (40x, 100x, 200x, and 400x). Fig 2 and 3 show slides of malignant and benign breast tumor. The total number of microscopic slides is 7909 (1995, 2081, 2013, and 1820 with respect to the abovementioned magnification factors). 652, 644, 623, and 588 of these images are benign (total 2480), and 1370, 1437,1390, and 1232 are malignant (total 5429).

3.2 Experimental setup and performance evaluation

We follow the protocol used in [38], where the dataset is divided into 70% training data and 30% testing data. This protocol is applied independently to each of the four totally different magnifications in terms of image and patient levels.

For the image level, the image recognition rate (IRR) is calculated as

$$\mathrm{IRR} = \frac{C_{rec}}{C_{Total}} \quad (3)$$

where C_Total is the total number of test cancer images, and C_rec is the number of cancer images that are properly classified.

Patient recognition rate (PRR) is calculated as

$$\mathrm{PRR} = \frac{\sum \mathrm{PS}}{\text{Total Number of Patient}} \quad (4)$$

ISSN: 1992-8645 www.jatit.org E-ISSN: 1817-3195

PS denotes to the patient score, which is calculated as

$$PS = \frac{C_{rec}}{C_N} \quad (5)$$

where $C_N$represents the number of cancer images of patients, whereas C_{rec}represents the number of cancer images that are properly classified.

For the pre-trained CNN, we explore the various pre-trained VGG group models such as Chatfield, verydeep16, and Googlenet. 1) VGGm model [39], for number of layers in this model, and convoluation filters, additionally to the dimension of those filters, I follow [40].

For the extra network, we train it by following the recommendations of [41] by adjusting dropout probability p to 0.5. Within the hidden layer, we use a sigmoid activation function. In addition to the backpropagation algorithm, the parameters are set according to [40].

Our results are obtained from three different pretrained CNN models: Vgg_m, VeryDeep_16, and Googlenet. To present our results, we consider two different scenarios regarding the dependency of magnification, the experiment was repeated five times and we take the average results of these experiments. In the first scenario (magnification dependent), we train CNN networks for each magnification factor separately. In the second scenario, we use all available data in the training set regardless of magnification. For each scenario, the results are compared at both patient and image levels.

3.3 Magnification Dependent Results

The accuracy of the proposed CNN methods for the first scenario (magnification dependent) are reported in Tables 1 and 2 for image and patient level, respectively. Table 1 shows the superiority of our obtained accuracy against all of the proposed state of the art methods at image level at several magnification factors.

Table 1: Recognition Rate (based on Image Level) (%)

Pretrained CNN	Magnification				Average
	40x	100x	200x	400x	
[9]	89.6±6.5	85.0±4.8	82.8±2.1	80.2±3.4	84.40
[38]	82.8±3.6	80.7±4.9	84.2±1.6	81.2±3.6	82.23
[42]	84.6±2.9	84.8±4.2	84.2±1.7	81.6±3.7	83.80
Proposed [a]	84.1±1.8	85.6±1.9	87.5±0.3	84.9±1.0	83.65
Proposed [b]	91.1±1.1	91.6±0.5	92.7±1.1	90.5±1.2	91.46
Proposed [c]	90.4±1.2	91.8±0.9	92.5±1.2	90.7±1.4	91.36

[a] Using Googlenet Pretrained CNN
[b] Using Very deep 16 Pretrained CNN
[c] Using Vgg_m Pretrained CNN

Table 2: Recognition Rate (based on Patient Level) (%)

Pretrained CNN	Magnification				Average
	40x	100x	200x	400x	
[38]	83.8±2.0	82.1±4.9	85.1±3.1	82.3±3.8	83.33
[9]	88.6±5.6	84.5±2.4	85.3±3.8	81.7±4.9	85.03
[42]	84.0±6.9	83.9±5.9	86.3±3.5	82.1±2.4	84.08
[43]	83.1±2.1	83.2±3.5	84.6±2.7	82.1±4.4	83.25
[40]	86.3±2.7	87.5±2.4	87.1±3.6	86.4±1.7	86.83
Proposed a	83.5±2.1	83.8±3.0	86.1±2.1	83.0±1.4	84.10
Proposed b	87.0±2.7	87.8±2.2	86.8±3.5	86.1±2.1	86.93

3.4 Magnification Independent Results

We further suggest the use of deep learning to meet the variety of appearances of breast cancer in histopathological images. CNN models have high capacities for diverse feature representation.

For training the CNN model, we used the BreaKHis training set independent of magnifications factors.

Tables 3 and 4 report the accuracy of the proposed CNN methods for the second scenario (magnification independent); they show that we still achieve better results than state of the art methods. All pre-trained CNN models achieve an accuracy better than state of the art results.

Table 3: Independent Recognition Rate (based on Patient Level) (%)

Pretrained CNN	Magnification				Average
	40x	100x	200x	400x	
[43]	83.1±2.1	83.2±3.5	84.6±2.7	82.1±4.4	83.25
Proposed [a]	84.1±1.5	84.5±2.5	86.3±2.2	84.8±2.4	84.94
Proposed [b]	86.1±3.2	86.8±2.6	88.0±2.7	85.9±1.4	86.71
Proposed [c]	86.4±1.9	87.5±2.1	86.6±2.6	86.1±2.6	86.64

ISSN: 1992-8645 www.jatit.org E-ISSN: 1817-3195

Table 4: Independent Recognition Rate (based on Image Level) (%)

Pretrained CNN	Magnification				Average
	40x	100x	200x	400x	
Proposed [a]	86.51±0.5	87.2±1.0	89.5±0.8	87.2±0.8	87.57
Proposed [b]	93.3±0.5	93.3±1.0	94.8±0.8	91.9±0.9	93.34
Proposed [c]	92.2±0.4	94.0±0.5	94.7±0.2	92.2±0.2	93.27

3.5 Comparison with state of the art methods

In this section, we compare our results to the ones available in the state of the art in two different scenarios. The recognition rate in the first scenario is magnification dependent, in the terms of Patient level, and image level, the second one is magnification independent at patient level. For both scenarios, we demonstrate superior results compared to state of the art methods.

In the first scenario, as shown in tables 1 and 2, the Average results of the Recognition Rate for the method proposed in [9] equal to (84.4%, and 85.0%) in image level and patient level respectively, while the results obtained in [42], are equal to (83.8%, and 84%), in image level and patient level respectively. The average of proposed results in the three different pre-trained models in the terms of image and patient level are (83.7%,84.1%) in Googlenet Pretrained CNN, and (91.5%, and 86.9%). Finally, by using Vgg_m Pretrained CNN in the image level, we get an average (91.4%) which is better than relevant literature. As we can see CNN_Very deep 16 and CNN_Vgg_m were able to achieve an accuracy approximately 1 – 10.5% higher than in previous works.

While in the second scenario as shown in Table 3, the obtained results in the three different pre-trained CNN models are better than the state of the art.

4 CONCLUSIONS

In this paper, we proposed a framework for the detection and classification of cancer in histopathological images. We used deep learning to meet the diversity of appearances of breast cancer in histopathological images. The achieved results show that the proposed deep learning method is better than state of the art methods. We evaluated the method in two different scenarios, and achieved results better than the state of the art. On the latter point, computer vision literature reports deep models designated for 'local' object detection in images as well as deep models for 'holistic' scene recognition. Thus, integrating both object-scene levels in the context of breast cancer diagnosis can effectively help in distinguishing benign from malignant cases as they manifest distinct local and global image attributes.

5 ACKNOWLEDGMENT

The authors thank the Deanship of Scientific Research and RSSU at King Saud University for their technical support and for its funding this Research Group No. (RG -1435-050).

REFERENCES:

[1] Y. LeCun, Y. Bengio, and G. Hinton, "Deep learning," Nature, vol. 521, no. 7553, pp. 436–444, May 2015.

[2] X. Li, Y. Yang, Z. Pang, and X. Wu, "A comparative study on selecting acoustic modeling units in deep neural networks based large vocabulary Chinese speech recognition," Neurocomputing, vol. 170, pp. 251–256, Dec. 2015.

[3] M. Cai and J. Liu, "Maxout neurons for deep convolutional and LSTM neural networks in speech recognition," Speech Communication, vol. 77, pp. 53–64, Mar. 2016.

[4] Z. Huang, R. Wang, S. Shan, and X. Chen, "Face recognition on large-scale video in the wild with hybrid Euclidean-and-Riemannian metric learning," Pattern Recognition, Mar. 2015.

[5] Q.-Q. Tao, S. Zhan, X.-H. Li, and T. Kurihara, "Robust face detection using local CNN and SVM based on kernel combination," Neurocomputing, vol. 211, pp. 98–105, Oct. 2016.

[6] Z. Jiao, X. Gao, Y. Wang, and J. Li, "A deep feature based framework for breast masses classification," Neurocomputing, vol. 197, pp. 221–231, Jul. 2016.

[7] W. Sun, T.-L. (Bill) Tseng, J. Zhang, and W. Qian, "Enhancing deep convolutional neural network scheme for breast cancer diagnosis with unlabeled data," Computerized Medical Imaging and Graphics.

[8] S. Albarqouni, C. Baur, F. Achilles, V. Belagiannis, S. Demirci, and N. Navab, "AggNet: Deep Learning From Crowds for Mitosis Detection in Breast Cancer Histology Images," IEEE Transactions on Medical Imaging, vol. 35, no. 5, pp. 1313–1321, May 2016.

[9] F. A. Spanhol, L. S. Oliveira, C. Petitjean, and L. Heutte, "Breast cancer histopathological image classification using Convolutional Neural Networks," in 2016 International Joint Conference on Neural Networks (IJCNN), 2016, pp. 2560–2567.

[10] K. Sirinukunwattana, S. E. A. Raza, Y. W. Tsang, D. R. J. Snead, I. A. Cree, and N. M. Rajpoot, "Locality Sensitive Deep Learning for Detection and Classification of Nuclei in Routine Colon Cancer Histology Images," IEEE Transactions on Medical Imaging, vol. 35, no. 5, pp. 1196–1206, May 2016.

ISSN: 1992-8645 www.jatit.org E-ISSN: 1817-3195

[11] J. Xu et al., "Stacked Sparse Autoencoder (SSAE) for Nuclei Detection on Breast Cancer Histopathology Images," IEEE Transactions on Medical Imaging, vol. 35, no. 1, pp. 119–130, Jan. 2016.

[12] T. Wan, J. Cao, J. Chen, and Z. Qin, "Automated grading of breast cancer histopathology using cascaded ensemble with combination of multi-level image features," Neurocomputing, vol. 229, pp. 34–44, Mar. 2017.

[13] R. Rouhi, M. Jafari, S. Kasaei, and P. Keshavarzian, "Benign and malignant breast tumors classification based on region growing and CNN segmentation," Expert Systems with Applications, vol. 42, no. 3, pp. 990–1002, Feb. 2015.

[14] A. M. Abdel-Zaher and A. M. Eldeib, "Breast cancer classification using deep belief networks," Expert Systems with Applications, vol. 46, pp. 139–144, Mar. 2016.

[15] Q. Zhang et al., "Deep learning based classification of breast tumors with shear-wave elastography," Ultrasonics, vol. 72, pp. 150–157, Dec. 2016.

[16] J. Arevalo, F. A. González, R. Ramos-Pollán, J. L. Oliveira, and M. A. Guevara Lopez, "Representation learning for mammography mass lesion classification with convolutional neural networks," Computer Methods and Programs in Biomedicine, vol. 127, pp. 248–257, Apr. 2016.

[17] F. Jiang et al., "Abdominal adipose tissues extraction using multi-scale deep neural network," Neurocomputing.

[18] M. Havaei et al., "Brain tumor segmentation with Deep Neural Networks," Medical Image Analysis, vol. 35, pp. 18–31, Jan. 2017.

[19] X. W. Gao, R. Hui, and Z. Tian, "Classification of CT brain images based on deep learning networks," Computer Methods and Programs in Biomedicine, vol. 138, pp. 49–56, Jan. 2017.

[20] J. Kleesiek et al., "Deep MRI brain extraction: A 3D convolutional neural network for skull stripping," NeuroImage, vol. 129, pp. 460–469, Apr. 2016.

[21] K. Kamnitsas et al., "Efficient multi-scale 3D CNN with fully connected CRF for accurate brain lesion segmentation," Medical Image Analysis, vol. 36, pp. 61–78, Feb. 2017.

[22] C. Spampinato, S. Palazzo, D. Giordano, M. Aldinucci, and R. Leonardi, "Deep learning for automated skeletal bone age assessment in X-ray images," Medical Image Analysis, vol. 36, pp. 41–51, Feb. 2017.

[23] M. M. A. Rahhal, Y. Bazi, H. AlHichri, N. Alajlan, F. Melgani, and R. R. Yager, "Deep learning approach for active classification of electrocardiogram signals," Information Sciences, vol. 345, pp. 340–354, Jun. 2016.

[24] S. Kiranyaz, T. Ince, and M. Gabbouj, "Real-Time Patient-Specific ECG Classification by 1-D Convolutional Neural Networks," IEEE Transactions on Biomedical Engineering, vol. 63, no. 3, pp. 664–675, Mar. 2016.

[25] P. Xiong, H. Wang, M. Liu, S. Zhou, Z. Hou, and X. Liu, "ECG signal enhancement based on improved denoising auto-encoder," Engineering Applications of Artificial Intelligence, vol. 52, pp. 194–202, Jun. 2016.

[26] A. Jemal et al., "Cancer statistics, 2008," CA Cancer J Clin, vol. 58, no. 2, pp. 71–96, Apr. 2008.

[27] H. Chougrad, H. Zouaki, and O. Alheyane, "Deep Convolutional Neural Networks for breast cancer screening," Computer Methods and Programs in Biomedicine, vol. 157, pp. 19–30, Apr. 2018.

[28] L. Adepoju, W. Qu, V. Kazan, M. Nazzal, M. Williams, and J. Sferra, "The evaluation of national time trends, quality of care, and factors affecting the use of minimally invasive breast biopsy and open biopsy for diagnosis of breast lesions," Am. J. Surg., vol. 208, no. 3, pp. 382–390, Sep. 2014.

[29] J. M. Eberth et al., "Surgeon Influence on Use of Needle Biopsy in Patients With Breast Cancer: A National Medicare Study," JCO, vol. 32, no. 21, pp. 2206–2216, Jul. 2014.

[30] M. Kowal, P. Filipczuk, A. Obuchowicz, J. Korbicz, and R. Monczak, "Computer-aided diagnosis of breast cancer based on fine needle biopsy microscopic images," Computers in Biology and Medicine, vol. 43, no. 10, pp. 1563–1572, Oct. 2013.

[31] P. Filipczuk, T. Fevens, A. Krzyżak, and R. Monczak, "Computer-Aided Breast Cancer Diagnosis Based on the Analysis of Cytological Images of Fine Needle Biopsies," IEEE Transactions on Medical Imaging, vol. 32, no. 12, pp. 2169–2178, Dec. 2013.

[32] Y. M. George, H. H. Zayed, M. I. Roushdy, and B. M. Elbagoury, "Remote Computer-Aided Breast Cancer Detection and Diagnosis System Based on Cytological Images," IEEE Systems Journal, vol. 8, no. 3, pp. 949–964, Sep. 2014.

[33] A. Krizhevsky, I. Sutskever, and G. E. Hinton, "ImageNet Classification with Deep Convolutional Neural Networks," in Advances in Neural Information Processing Systems 25, F. Pereira, C. J. C. Burges, L. Bottou, and K. Q. Weinberger, Eds. Curran Associates, Inc., 2012, pp. 1097–1105.

[34] C. Farabet, C. Couprie, L. Najman, and Y. LeCun, "Learning Hierarchical Features for Scene Labeling," IEEE Transactions on Pattern Analysis and Machine Intelligence, vol. 35, no. 8, pp. 1915–1929, Aug. 2013.

[35] P. Sermanet, D. Eigen, X. Zhang, M. Mathieu, R. Fergus, and Y. LeCun, "OverFeat: Integrated Recognition, Localization and Detection using Convolutional Networks," Dec. 2013.

[36] N. Srivastava, G. Hinton, A. Krizhevsky, I. Sutskever, and R. Salakhutdinov, "Dropout: A Simple Way to Prevent Neural Networks from Overfitting," Journal of Machine Learning Research, vol. 15, pp. 1929–1958, 2014.

[37] E. Othman, Y. Bazi, F. Melgani, H. Alhichri, N. Alajlan, and M. Zuair, "Domain Adaptation Network for Cross-Scene Classification," IEEE Transactions on

ISSN: 1992-8645 www.jatit.org E-ISSN: 1817-3195

Geoscience and Remote Sensing, vol. 55, no. 8, pp. 4441–4456, Aug. 2017.

[38] F. A. Spanhol, L. S. Oliveira, C. Petitjean, and L. Heutte, "A Dataset for Breast Cancer Histopathological Image Classification," IEEE Transactions on Biomedical Engineering, vol. 63, no. 7, pp. 1455–1462, Jul. 2016.

[39] K. Simonyan and A. Zisserman, "Very Deep Convolutional Networks for Large-Scale Image Recognition," Sep. 2014.

[40] M. M. A. Rahhal, "Breast Cancer Classification in Histopathological Images using Convolutional Neural Network," International Journal of Advanced Computer Science and Applications (IJACSA), vol. 9, no. 3, 2018.

[41] Y. Bengio, A. Courville, and P. Vincent, "Representation Learning: A Review and New Perspectives," IEEE Transactions on Pattern Analysis and Machine Intelligence, vol. 35, no. 8, pp. 1798–1828, 2013.

[42] F. A. Spanhol, L. S. Oliveira, P. R. Cavalin, C. Petitjean, and L. Heutte, "Deep features for breast cancer histopathological image classification," in 2017 IEEE International Conference on Systems, Man, and Cybernetics (SMC), 2017, pp. 1868–1873.

[43] Neslihan Bayramoglu, Juho Kannala, and Janne Heikkilä, "Deep Learning for Magnification Independent Breast Cancer Histopathology Image Classification," in 23rd International Conference on Pattern Recognition, 2016.